Military Technical College
Kobry El-Kobbah,
Cairo, Egypt.

13th International Conference on Applied Mechanics and Mechanical Engineering.

THE TRANSITION FROM SINGLE TO MULTIPLE CRACKING IN CERAMIC/METAL LAMINATES

El-Shaer* Y. and Derby** B.

ABSTRACT

During the fracture of metal/ceramic laminates two different damage modes are observed: one is the formation of a zone of multiple cracks near the tip of a macroscopic crack, and the other is the continuous propagation of a macroscopic crack in the ceramic layers while the metal layers remain intact. The criterion for the transition from single to multiple cracking is a key parameter for the design of metal/ceramic laminates. A plot (which is called a 'Fracture map') has been constructed to enable the designer to determine the fracture mode for a given laminate.

In the present work, a new fracture map is proposed which includes the effect of the non-deterministic strength of the ceramic on the transition from single to multiple cracking. The proposed probability-based fracture map is compared with previous maps, and compared with experimentally observed fracture modes of different ceramic/metal laminates.

KEY WORDS

Ceramic, Crack growth, Laminates, Fracture.

* Egyptian Armed Forces.
** Professor, Manchester Materials Science Centre, UMIST, Manchester, U.K.

INTRODUCTION

Ceramic materials have the advantage of good creep resistance, low density, excellent wear resistance, and chemical inertness, which make them suitable for use in many applications. However, the use of ceramics in engineering applications is severely limited by their low toughness, which can cause catastrophic failure of the structure.

During the last decades, different toughening mechanisms have been discovered or developed, such as transformation toughening, micro cracking, whisker, platelet or ceramic fiber reinforcement and incorporation of a ductile metallic phase [1]. The ductile metallic phase approach promises the best of two worlds: the brittle matrix preserves stiffness and lightness; the metal phase enhances toughness and energy absorption capacity [2].

Numerous reinforcement shapes have been employed in various ductile-brittle composite systems, including particulate, fiber and laminate reinforcements. Early studies showed that fiber-reinforced composites generally promote greater levels of toughening than particulate-reinforced composites. However, subsequent work on ductile layer reinforced composites soon revealed that such composite architectures result in even greater levels of toughening than ductile fiber reinforced brittle matrix composites [3-5].

There are two different damage modes observed during the fracture of metal/ceramic laminates (Fig. 1): one is the formation of a zone of multiple cracks near the tip of a macroscopic crack, and the other is the continuous propagation of a macroscopic crack in the ceramic layers while the metal layers remain intact. As the criterion for the transition from single to multiple cracking is a key parameter for the design of metal/ceramic laminates, this subject has been investigated by many authors[6-11]. Fracture maps have been constructed to enable the designer to determine the fracture mode for a given laminate with certain given geometrical and mechanical properties of the ceramic and the metal layers. A typical fracture map is shown in Fig. 2.

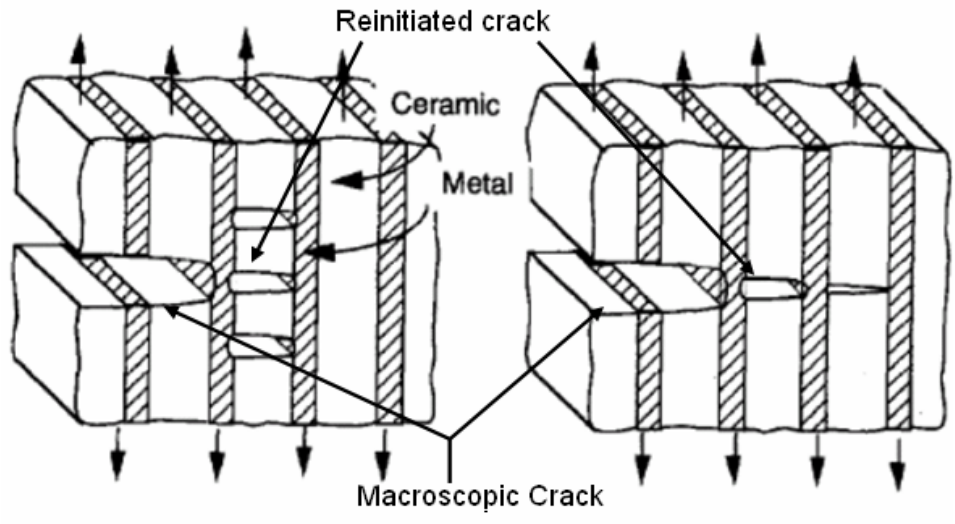

a) Multiple cracking **b) Single cracking**

Fig. 1. Cracking modes in ceramic/metal laminate [7]

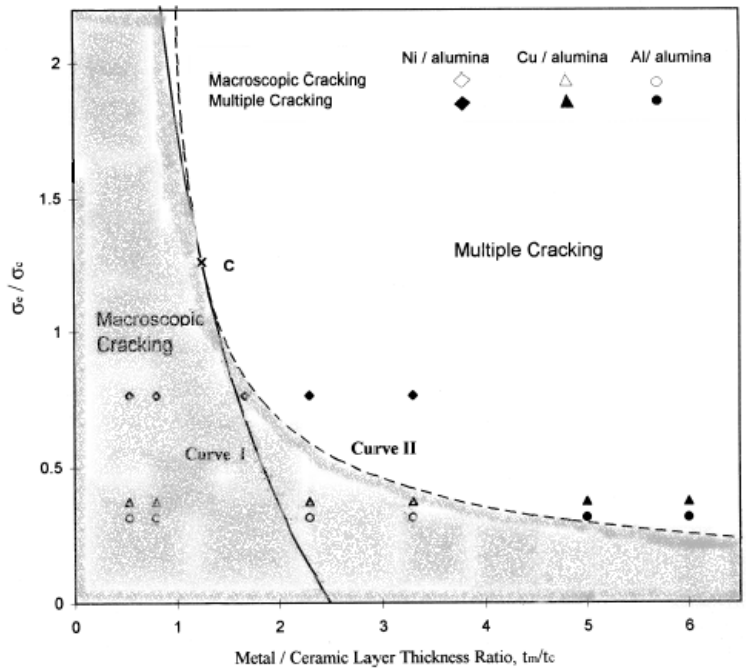

Fig. 2. Composite fracture map [9]

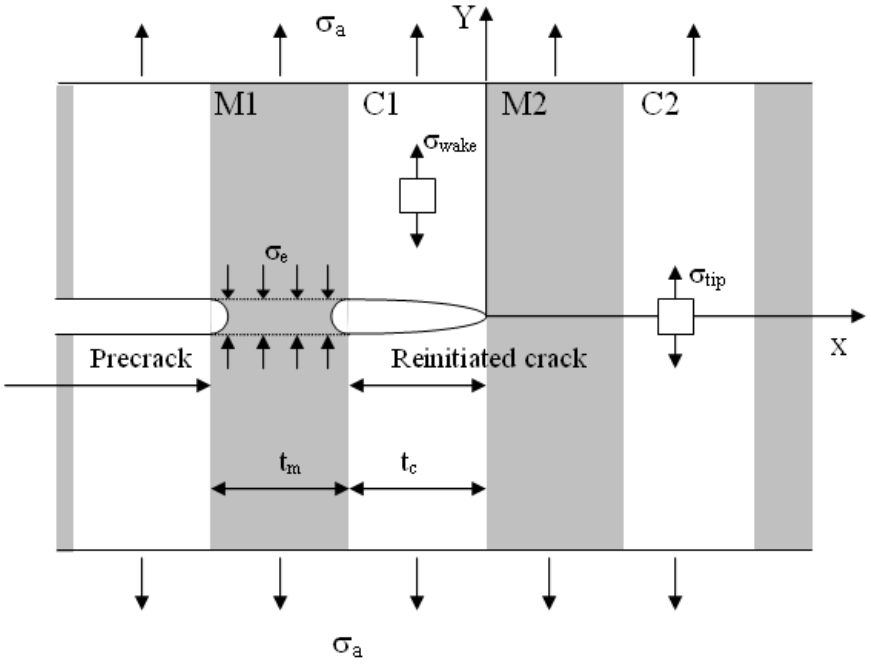

Fig. 3. Schematic representation of a cracked laminate with a bridging metal layer showing the location of the tip and wake stresses

TRANSITION FROM SINGLE TO MULTIPLE CRACKING

Factors affecting the transition from single to multiple cracking have been studied by many authors [6-11], and different fracture maps has been constructed to enable predicting the fracture mode for a given laminate with certain given geometrical and mechanical properties of the ceramic and the metal layers (Fig. 3). The main geometrical parameter, which affects the transition from single to multiple cracking

mode is the laminate thickness ratio, t_m / t_c (t_m and t_c are the metal and ceramic layers thickness respectively) while the mechanical properties include the ceramic fracture strength and the constrained yield stress of the metal layer.

Shaw et al. [6] developed a simple model to describe the transition from single to multiple cracking assuming an elastic homogeneous medium. The stresses in the wake and tip regions were calculated as an effect of two contributions: the K-field of the main crack tip, and the bridging traction exerted by the intact metal layer. The bridging traction has been assumed to have a constant value, and its effect on the wake stress distribution has been obtained using contact mechanics [12, 13]. The results show that for a ceramic laminate reinforced with a metal which has a sufficiently high yield strength, as the volume fraction of the metal increases, the location of the peak stress moves from the tip region to the wake. These results were consistent with their limited experimental results.

Huang et al. [10] studied the conditions that will facilitate the transition from single to multiple cracking using linear elastic fracture mechanics and the shear lag analysis. The Dugdale model [14] was applied to examine the effect of plasticity in the shear lag analysis. The effects of metal/ceramic layer thickness ratio, moduli, and plastic yielding and hardening on the competition between the multiple and single cracking modes were investigated. A critical thickness ratio, $(t_m/t_c)_{crit}$ was found above which multiple cracking dominates. This value is proportional to the corresponding moduli ratio, such that the competition between damage modes is governed by the ratio of the metal/ceramic layer stiffness, $(E_m t_m/E_c t_c)$. The plastic hardening of metals helps to activate the multiple cracking mode, (as it increase the bridging traction), while the plastic yielding does the opposite. Further work of Huang and Zhang [11] introduced a new parameter affecting the cracking mode, which is the ceramic fracture stress, σ_c. A fracture map was established, from which was concluded that as long as the metal layer thickness is 2.5 times larger than the ceramic layer thickness, $(t_m/t_c>2.5)$, multiple cracking always occurs for a well-bonded laminate, regardless of the metal/ceramic properties. However, the experimental results were not in complete agreement with their fracture map.

Hwu and Derby [9] studied the transition from single to multiple cracking for three metal/ceramic laminate systems with different metal to ceramic strength as a function of the metal/ceramic ratio. It was observed that the deviation between the experimental results and the model of Huang and Zhang is most pronounced when metals with low yield strength are used in the laminate, so this deviation was attributed to the influence of metal plasticity. A composite model was developed to include the effect of extensive plasticity, using the shear lag analysis at lower values of metal yield stresses, and linear elastic fracture mechanics at other values. This composite model agrees well with the experimental results as shown in Fig. 2.

Shaw et al. [7] used finite element modelling (FEM) to investigate the effect of metal plasticity on the transition between single to multiple cracking. The experimental observations of elastic and plastic strain distributions using moiré interferometry have been used to check the assumptions used in the FEM. A good agreement between experimental and predicted strain distributions was obtained, which indicates the validity of the assumptions used in the FEM. Using the maximum tip and wake stresses from FEM at different loads for each composite system, a fracture map was formulated.

The elastic mismatch between the ceramic and metal layers was neglected. Experimental results were in partial agreement with the developed fracture map.

In all the previous studies, the fracture strength of the ceramic was considered as a constant value (σ_c). Unfortunately, most experimental evidence indicates that brittle matrix cracking occurs continuously over a broad band of stresses, indicating that statistical aspects are important [15]. Thus, a probabilistic-based analysis has been developed by Shaw [8]. Shaw has developed a probabilistic analysis using the two-parameter Weibull equation, which is widely used to characterize the strength of brittle solids [2, 16]. The results from the probabilistic analysis were used to identify a boundary corresponding to the transition in fracture mode for multilayer systems (Fig. 4) with variable metal volume fraction, f, and Weibull modulus. This was accomplished by determining the magnitude of the critical Weibull modulus, m^*, at which point the probability of failure in the tip region (V_A) equals to the probability of failure in the rest of the ceramic volume (V_B) equals to certain failure probability (which was taken 0.5) for each volume fraction and specimen geometry:

$$P_f(V_A,\ \sigma_\infty^*) = P_f(V_A,\ \sigma_\infty^*) = 0.5$$

Then, the critical Weibull modulus is plotted against metal volume fraction, for different specimen geometry, giving the fracture map in Fig. 5.

We can see from the previous study that the composite model [9], in spite of its simplicity, was able to give excellent predictions with the experimental results for different ceramic/metal laminate systems (Alumina with Ni, Cu, and Al). However, it is not known yet if this model will be able to predict the failure mode for other ceramic laminate systems, when the difference in modulus of elasticity is very high.

Another aspect is the non-deterministic strength of ceramics, which was studied by Shaw [8]. The previous probabilistic-based analysis is not examined yet with sufficient experimental data. It is important also, to check whether the Weibull parameters of the ceramic will change due to processing of the laminate. Such a change was observed in the case of brittle fibres [15]. It is also required to modify the basis of the probabilistic approach to be suitable for application in the case of bending test specimens, as it was deduced mainly for the case of uniform applied remote stress.

The objective of the present work is to improve the predictive capabilities of the current analytical models used to predict whether the fracture occurs by the propagation of a low energy single dominant crack or by high energy dissipating multiple cracking within each ceramic layer. Of particular importance is the need to verify the analytical predictions experimentally using a wide range of ceramic-ductile phase combinations. A probability-based fracture map has been constructed using LEFM and Weibull statistics. Experimental results obtained from laminates with different combinations of ceramics and metals have been used to assess the new map and compare it with the composite model explained before [9].

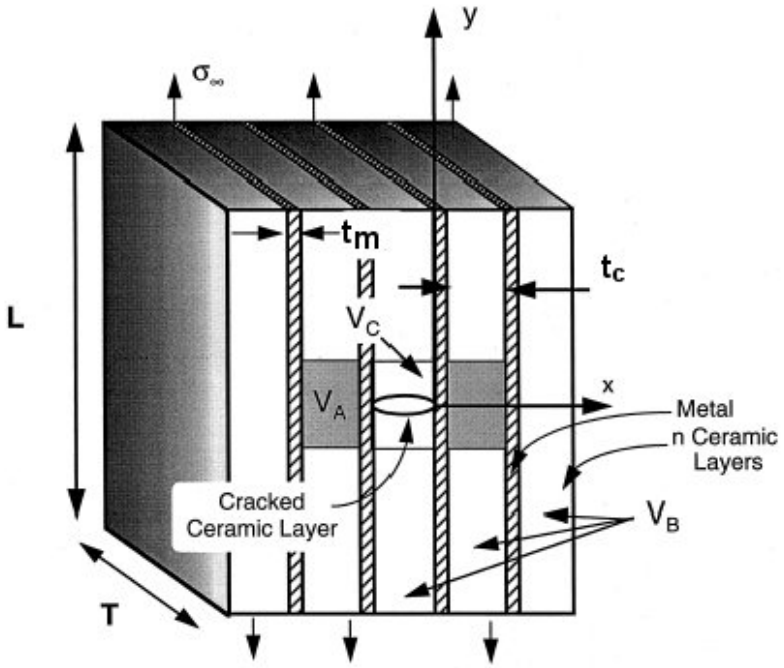

Fig. 4. The specimen used in the probabilistic analysis [8].

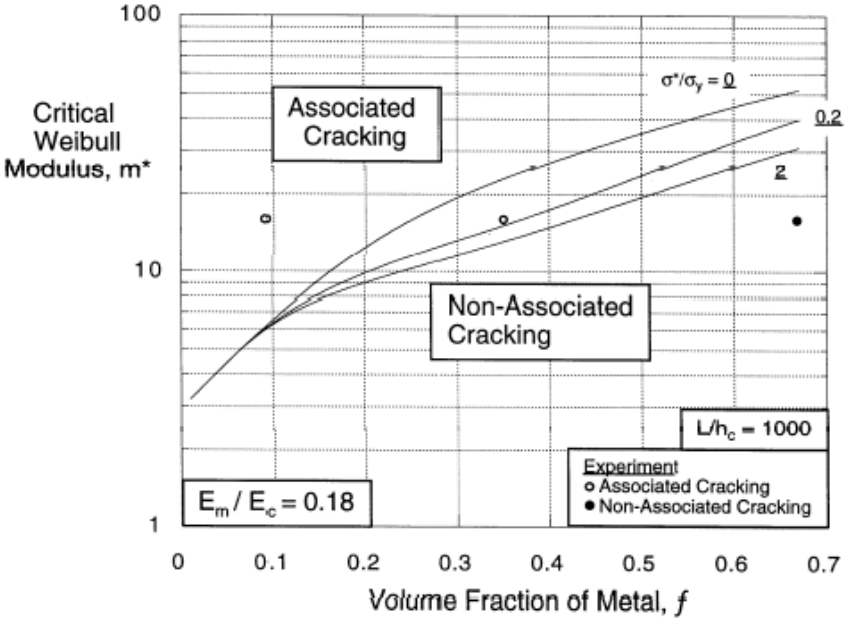

Fig. 5. Probabilistic based fracture map [8]

MODELLING OF THE TRANSITION FROM SINGLE TO MULTIPLE CRACKING

For the cracked laminate shown in Fig. 6, assuming an elastic homogeneous medium, the stresses in the ceramic layers C_1 and C_2 were obtained based on linear elastic fracture mechanics (LEFM) [6]. The stresses were calculated as an effect of two contributions: the K-Field of the main crack tip, (K_{net}), and the bridging traction exerted by the intact metal layer. The bridging traction was assumed to have a constant value (σ_e), and its effect on the wake stress distribution was obtained using contact mechanics [12, 13].

$$\sigma_{tip}(x,y) = \frac{K_{net}}{\sqrt{2\pi r}} . f_{yy}(\theta) \tag{1}$$

$$\sigma_{wake}(x,y) = \frac{K_{net}}{\sqrt{2\pi r}} f_{yy}(\theta) + \frac{\sigma_e}{\pi}(\alpha + \sin\alpha\cos\phi) \tag{2}$$

where

$$r = \sqrt{x^2 + y^2}\ ,\ \theta = \arctan(y/x),\ f_{yy}(\theta) = \cos(\theta/2)[1 + \sin(\theta/2)\sin(3\theta/2)]$$

$$\alpha\left(\frac{t_m}{t_c}, \frac{y}{t_c}, \frac{x}{t_c}\right) = \arctan\left(\frac{\frac{t_m}{t_c} + 1 - \left|\frac{x}{t_c}\right|}{\frac{y}{t_c}}\right) - \arctan\left(\frac{1 - \left|\frac{x}{t_c}\right|}{\frac{y}{t_c}}\right)$$

$$\phi\left(\frac{t_m}{t_c}, \frac{y}{t_c}, \frac{x}{t_c}\right) = \arctan\left(\frac{\frac{t_m}{t_c} + 1 - \left|\frac{x}{t_c}\right|}{\frac{y}{t_c}}\right) + \arctan\left(\frac{1 - \left|\frac{x}{t_c}\right|}{\frac{y}{t_c}}\right)$$

The stress variation parallel to crack in each ceramic layer is small, as the layer thickness is small compared to the pre-crack length. As a result, the stress in each ceramic layer is well approximated by its average over the ceramic layer thickness[9, 11]. Equations (1) and (2) are changed to:

$$\sigma_{tip}(y) = \frac{1}{t_c}\int_{t_m}^{t_m + t_c} \frac{K_{net}}{\sqrt{2\pi x}}\, dx \tag{3}$$

$$\sigma_{wake}(y) = \frac{1}{t_c}\left\{\int_{-tc}^{0}\left[\frac{K_{net}}{\sqrt{2\pi r}} f_{yy}(\theta) + \frac{\sigma_e}{\pi}(\alpha + \sin\alpha\cos\phi)\right] dx\right\} \tag{4}$$

A model has been developed taking into consideration the non-deterministic strength of the ceramic materials. For a cracked ceramic-metal laminate, assuming an elastic homogeneous medium The stress distribution in the wake and tip regions (σ_{wake} and σ_{tip} respectively) can be obtained based on linear elastic fracture mechanics using the same equations shown before (3 and 4).

The two-parameter Weibull equation is widely used to characterize the strength of brittle solids [2,16]. This description is based on the fact that the fracture stress of brittle

materials is a statistical quantity. The probability of failure $P_f(V,\sigma)$ of any brittle material of volume V, subjected to a local tensile stress, σ, is given by:

$$P_f(V,\sigma) = 1 - \exp\left[-\left(\frac{V}{V_o}\right)\left(\frac{\sigma}{\sigma_o}\right)^m\right] \quad (5)$$

where σ_o is the average strength of a given volume V_o , and m is the Weibull modulus of strength distribution.

The failure probability of structures that are subject to complex stress distributions $\sigma(x, y, z)$ is given by

$$P_f(V, \sigma(x, y, z)) = 1\text{-}\exp\left[-\left(\frac{1}{V_o\sigma_o^m}\right)\int_V \{\sigma(x,y,z)\}^m dV\right] \quad (6)$$

In our case, we have two volumes of interest are the wake region and the tip region. It is assumed that a crack will be initiated within one of the ceramic layers when the probability of failure reaches a critical value, P_f^{cr} ($P_f(V_{wake},\sigma_{wake}) = P_f^{cr}$ or $P_f(V_{tip},\sigma_{tip}) = P_f^{Cr}$). By substituting the stress distribution ($\sigma_{tip}(x,y)$) from equation (3) into (6) and at the starting of failure ($P_f(V_{tip},\sigma_{tip}) = P_f^{cr}$), we can get the critical stress intensity factor (SIF) causing crack initiation in the tip region:

$$K_{net}^{cr} = \left(\frac{-\ln(1-P_f^{cr}).(V_o.{\sigma_c}^m)}{B.t_c\int_0^{y_{tip}}\left(\frac{1}{t_c}\int_{t_m}^{t_m+t_c}\left(\frac{f_{yy}(x,y)}{\sqrt{2\pi r(x,y)}}\right)dx\right)^m dy}\right)^{\frac{1}{m}} \quad (7)$$

Substituting with this critical SIF again for the wake region we get the probability of failure in the wake region.

$$P_f(V_{wake},\sigma_{wake}) = 1 - e^{\left(\frac{-1}{V_o{\sigma_c}^m}.B.t_c\left(\int_0^{y_{wake}}\left(\frac{1}{tc}\int_{-tc}^{0}\left(\frac{{K_{net}}^{cr}}{\sqrt{2\pi r}}f_{yy}(\theta)+\frac{\sigma_e}{\pi}(\alpha+\sin\alpha\cos\phi)\right)dx\right)^m\right)dy\right)} \quad (8)$$

If $P_f(V_{wake},\sigma_{wake}) > P_f^{cr}$ then it is most likely for multiple cracking to occur, otherwise single cracking is assumed to be the cracking mode. A critical Weibull modulus separating the two cracking modes obtained when: $P_f(V_{tip},\sigma_{tip}) = P_f(V_{wake},\sigma_{wake}) = P_f^{cr}$. Determination of the critical Weibull modulus for a 50% critical failure probability ($P_f^{cr} = 0.5$) is shown in Fig. 7.

The critical failure probability has been changed to different values (0.5, 0.7, 0.9) to study its effect on the predicted fracture map. As can be seen from Fig. 8, no significant effect is observed. A critical failure probability of 0.5 is used in the following predictions.

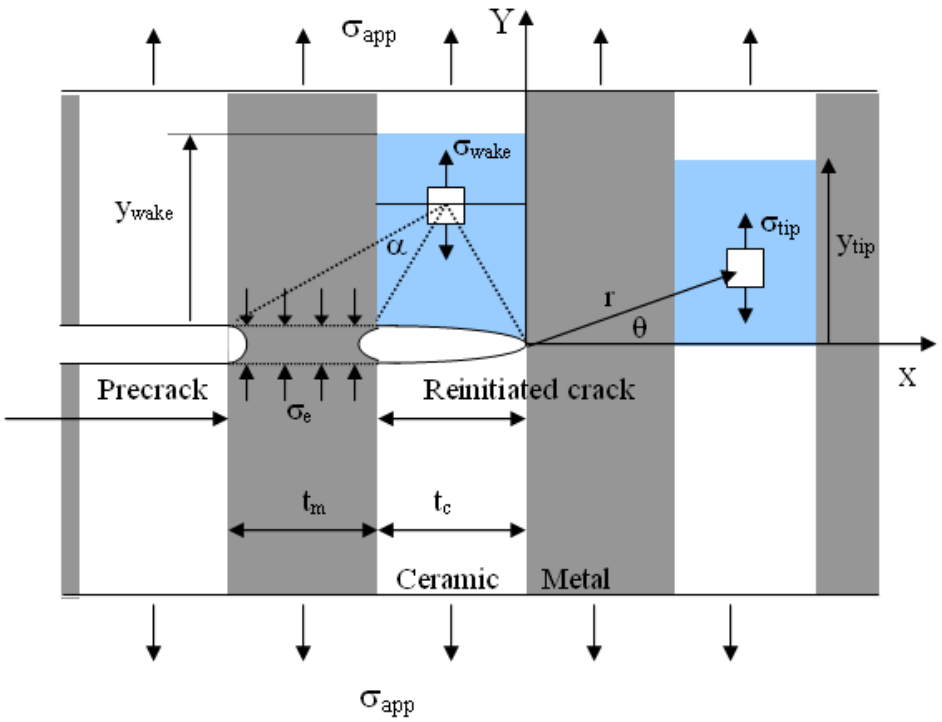

Fig. 6. Schematic representation of cracked ceramic-metal laminate with a bridging metal layer and the parameters used in the probability analysis

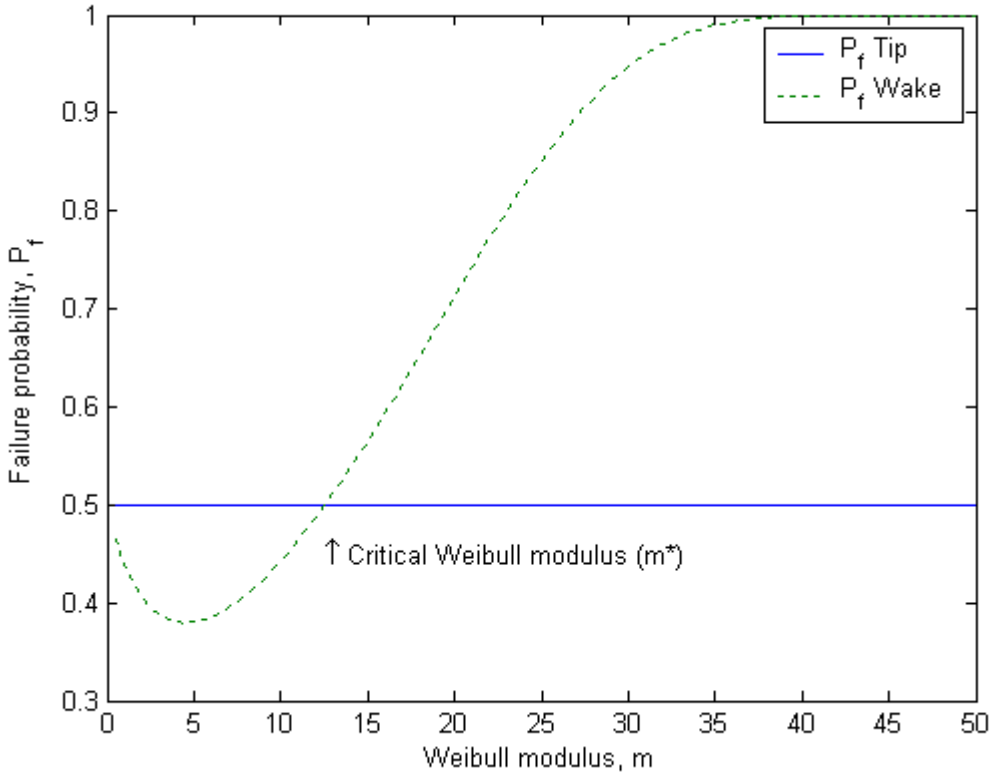

Fig. 7. Determination of the critical Weibull modulus m*

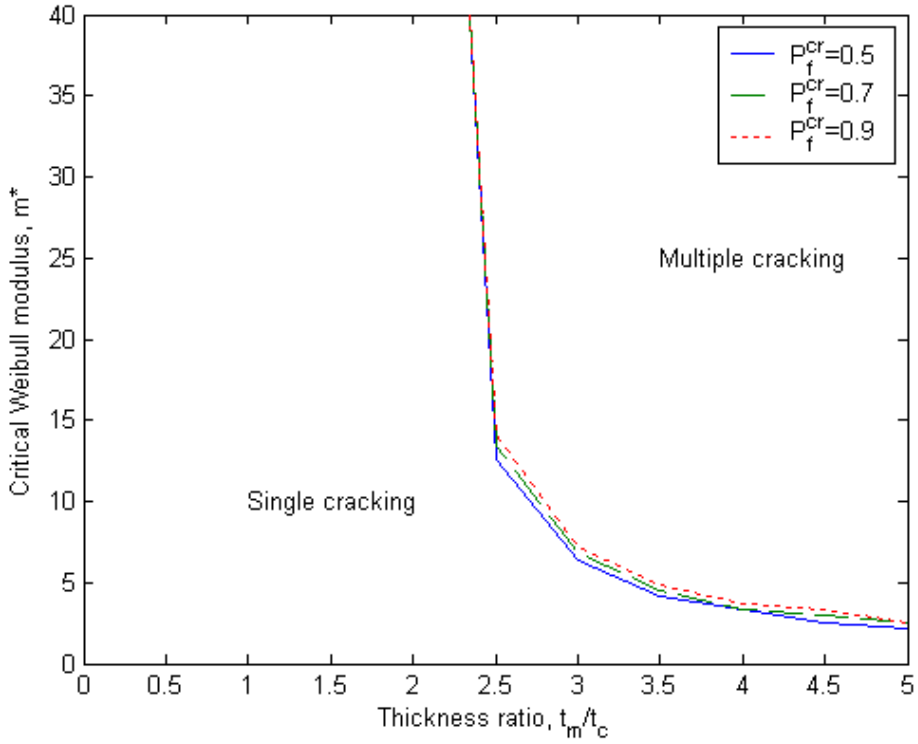

Fig. 8 Effect of critical failure probability (P_f^{cr}) on the predicted fracture map

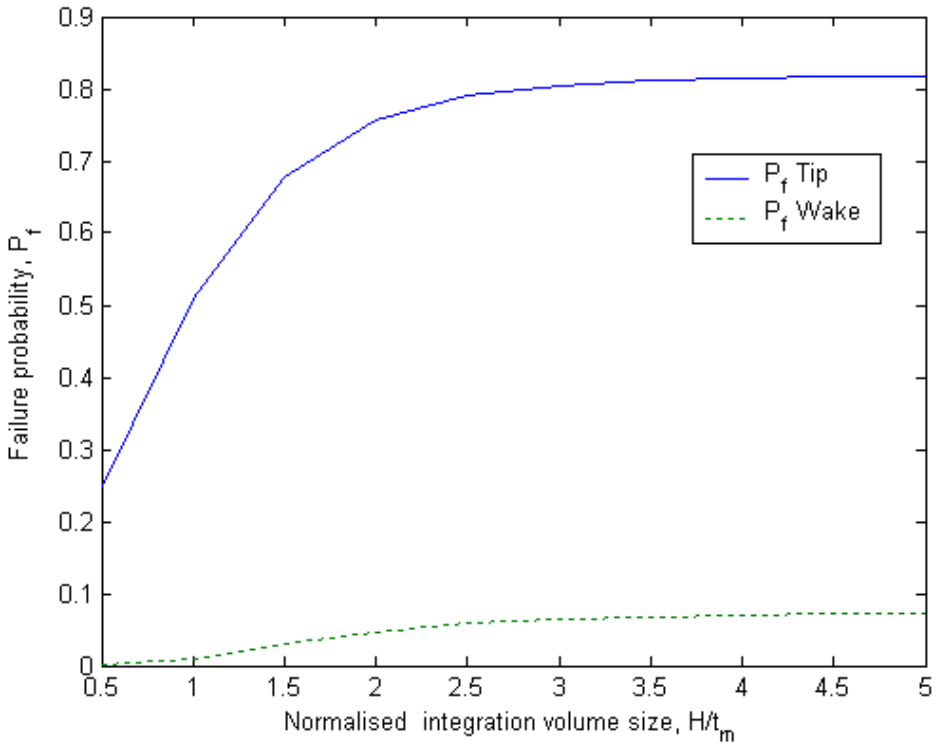

Fig. 9. Effect of integration volume on the failure probability in the tip and wake regions

To select the height of the wake and tip regions, which indicates the ceramic volume used in the Weibull analysis, the probability of failure in the wake and tip regions has been calculated for different values of the height as shown in Fig. 9. It can be seen the failure probability converged to a constant value at $H/t_m=3$, and this value is used for the calculations in the present probability based fracture map.

EXPERIMENTAL WORK

The fracture mode was examined using different combinations of tape-casted alumina and PSZ bonded to Aluminum and Nickel using diffusion bonding technique [18]. Typical combinations are listed in Table 1.

The specimen consists of nine ceramic layers and eight metal layers. A notch was cut traversing four intervening metal layers and rooted in the central ceramic layer. To be able to machine a well-defined notch for relatively thin ceramic sheets (<200μm), a thicker ceramic layer has been used in the middle and the outer layers.

A four-point bend fixture (Fig. 10) with inner and outer spans of 10 mm and 20 mm respectively has been used. Tests were executed using a bench-top testing machine (CK 10, Engineering Systems, Nottingham, UK) with 10 kN load cell. This machine has a built in acoustic sensor, which enables detection of crack propagation in the ceramic layer. The crack advance was also confirmed using a ×30 hand-held microscope. Loading was under displacement control condition, with a crosshead speed of 0.01 mm/min to ensure stable crack growth within the laminate. The cracking mode (single or multiple cracking) for the cracked ceramic/metal laminates was determined using optical microscopy.

Optical images of the different fracture patterns obtained are shown in Fig. 11. Most of the investigated ceramic/metal combinations fractured in single cracking mode, while the multiple cracking mode was only observed in three samples which are shaded in Table 1.

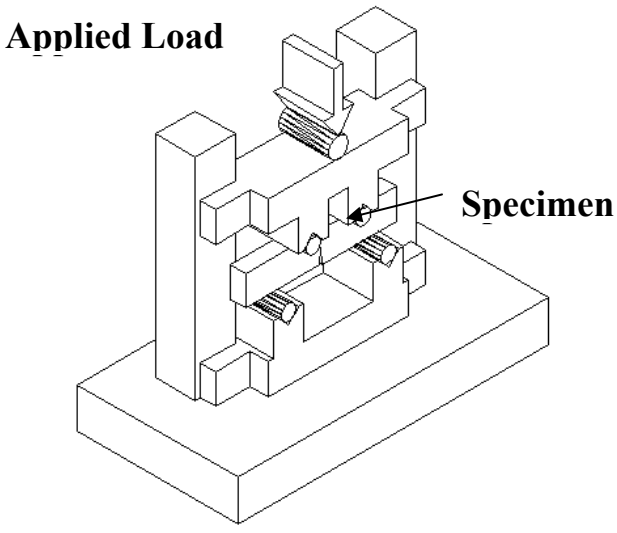

Fig. 10. Loading arrangement used in measuring fracture mode for ceramic-metal laminates.

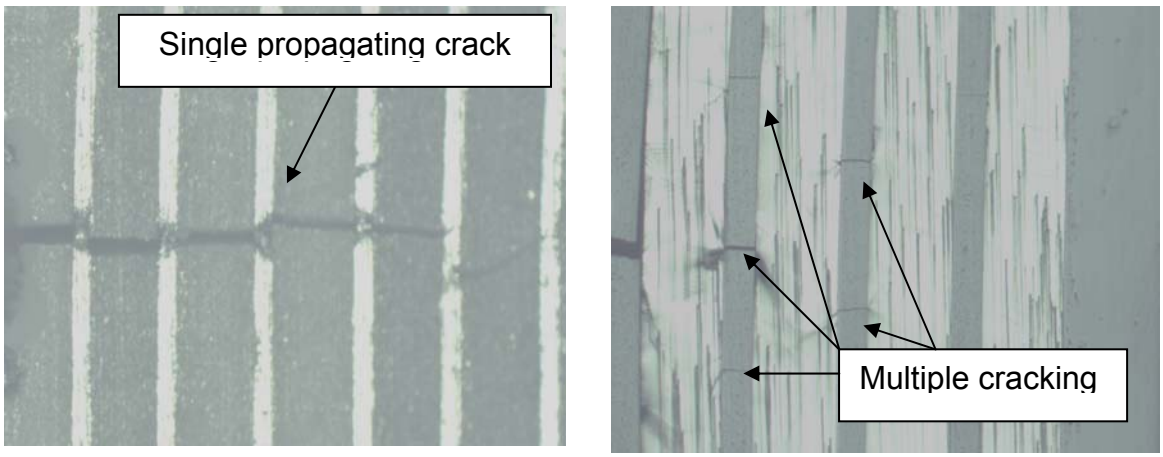

Fig. 11. Single and multiple cracking modes obtained for the tested laminates.

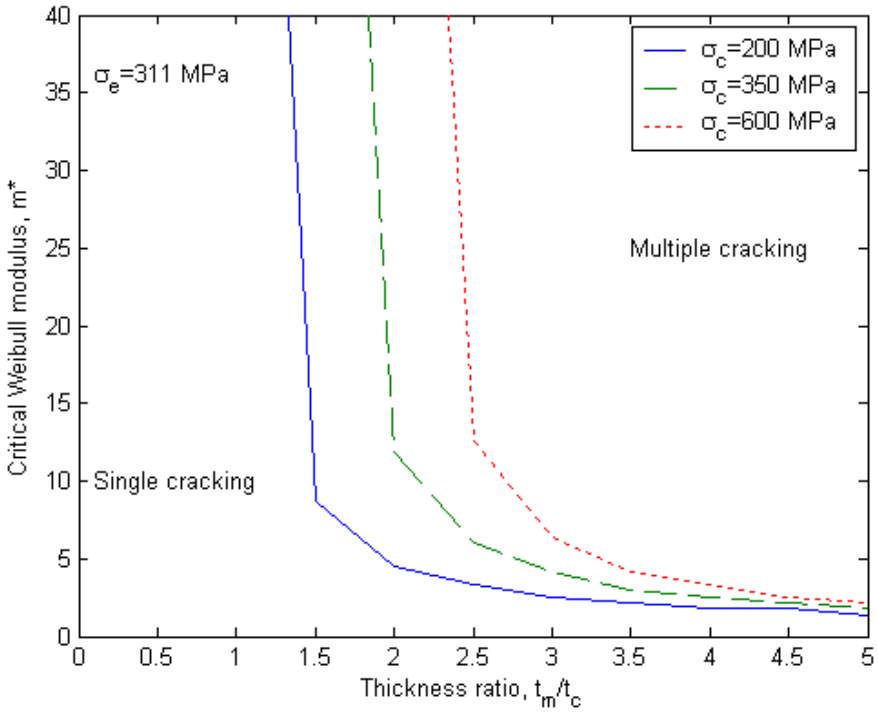

(a)

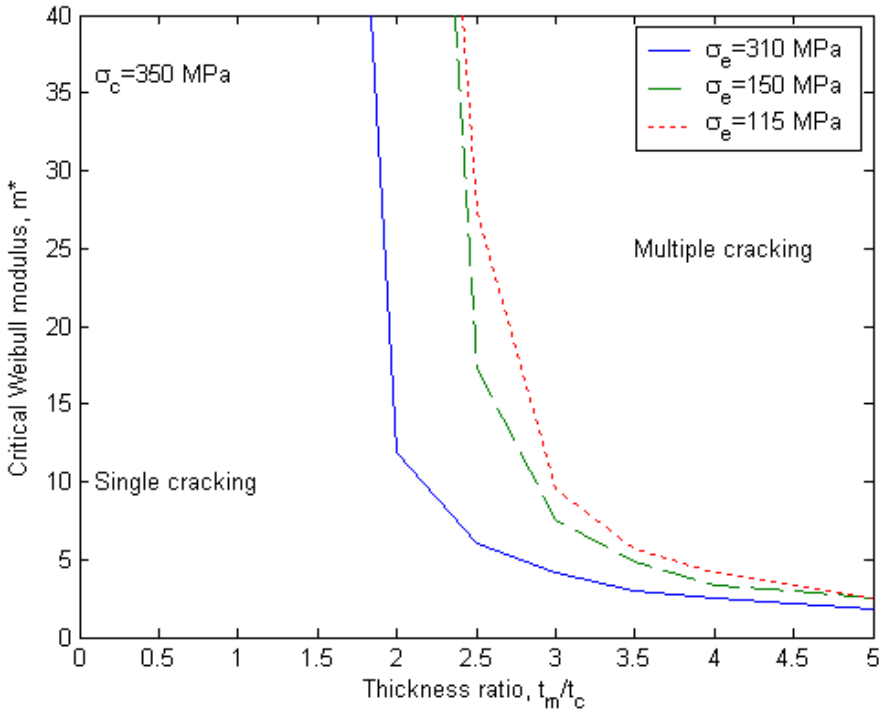

(b)

Fig. 12. Fracture map for ceramic-metal laminates, a) Ceramics with different fracture strengths, and b) Different bridging stresses

DISCUSSION AND CONCLUSIONS

Fracture maps for ceramic-metal laminates with different ceramic median strength and metal bridging stress are shown in Fig. 12 (a,b). As can be seen from Fig. 12-a, the tendency of multiple cracking to be the dominant cracking mode is decreased with the increase of the ceramic median strength, while this tendency is increased as the Weibull modulus and the metal bridging stress increase. Also, as the metal to ceramic thickness ratio (t_m/t_c) increases, it becomes much more probable for multiple cracking to occur rather than single cracking. These observations are generally in agreement with the previous results [6, 9, 11, 17].

These observations are in partial agreement with the fracture map (Fig. 5) proposed by Shaw [8] using finite element modeling to get the stress distribution within the laminate in the case of uniform applied stress. It was suggested that for the same metal volume fraction, increasing the Weibull modulus of the ceramic promotes the single cracking mode. However, in the present fracture map, there is a region where increasing the Weibull modulus results in multiple cracking to be the cracking mode of the laminate. Another aspect is the existence of a region of single cracking mode, which is not affected by the value of the Weibull modulus. This region was not observed in the fracture map proposed by Shaw.

For the experimental results obtained using different ceramic/metal laminates (Alumina and PSZ bonded to Nickel and Aluminium) with different metal to ceramic thickness

ratios (t_m/t_c=0.125:4) and different Weibull parameters for the strength of the ceramic layers (m=3:9.2), the probability-based map was able to predict the fracture mode of the ceramic/metal laminates more accurately than the modified composite map. These results support the basis used in the probability map formulation. However, it is recommended that the proposed map be investigated with more experimental results, especially near the boundary separating the single to multiple cracking transition.

REFERENCES

1. Raddatz, O., et al., Bridging stresses and R-curves in ceramic/metal composites. Journal of the European Ceramic Society, 2000. 20(13): p. 2261-2273.
2. Lawn, B., Fracture of Brittle solids. Second ed. 1993: Cambridge University Press.
3. Soboyejo, W.O., et al., Effect of reinforcement morphology on the fatigue and fracture behavior of MoSi2/Nb Composites. Acta Materialia, 1996. 44(5): p. 2027-2041.
4. Li, M., et al., An investigation of fracture behavior in layered NiAl/V composites. Scripta Materialia, 1999. 40(4): p. 397-402.
5. Li, M. and W.O. Soboyejo, An Investigation of the effects of ductile-Layer thickness on the fracture behavior of nickel aluminide microlaminates. Metallurgical and Materials Transactions A, 2000. 31A(5): p. 1385-1399.
6. Shaw, M.C., et al., Cracking and damage mechanisms in ceramic/metal multilayers. Acta metall. mater., 1993. 41(11): p. 3311-3322.
7. Shaw, M.C., et al., Cracking patterns in metal-ceramic laminates: effects of plasticity. Journal of the Mechanics and Physics of Solids, 1996. 44(5): p. 801-821.
8. Shaw, M.C., The effects of strength probabilistics on the fracture mode of ceramic/metal multilayers. Engineering Fracture Mechanics, 1998. 61(1): p. 49-74.
9. Hwu, K.L. and B. Derby, Fracture of metal/ceramic laminates-I. Transition from single to multiple cracking. Acta Materialia, 1999. 47(2): p. 529-543.
10. Huang, Y., H.W. Zhang, and F. Wu, Multiple cracking in metal-ceramic laminates. International Journal of Solids and Structures, 1994. 31(20): p. 2753-2768.
11. Huang, Y. and H.W. Zhang, The role of metal plasticity and interfacial strength in the cracking of metal/ceramic laminates. Acta Metall. Mater., 1995. 43(4): p. 1523-1530.
12. Roark, R.J. and W.C. Young, Formulas for stress and strain. Fifth ed. 1954, New York: McGraw-Hill. p.519.
13. Johnson, K.L., Contact Mechanics. 1985, Cambridge: Cambridge University Press. p. 21.
14. Dugdale, D.S., Yielding of steel sheets containing slits. J. Mech. Phys. Solids, 1960. 8: p. 100-104.
15. Curtin, W.A., Exact theory of fibre fragmentation in a single-filament composite. journal of Material Science, 1991. 26: p. 5239-5253.
16. Hull, D. and T.W. Clyne, An introduction to composite materials. second ed. 1996, Cambridge: Cambridge university press.
17. Hwu, K.L., Fracture studies of metal/ceramic laminates, in Materials. 1998, University of Oxford: Oxford. p. 118.
18. El-Shaer, Y., Fracture of Ceramic-Metal Laminates, in Materials Science Centre. 2003, UMIST: Manchester.

Table 1 Parameters of different laminates used in cracking mode investigation.

Properties	Ceramic			Metal		Laminate	
Sample-designation	t_c [μm]	σ_c [MPa]	m	t_m [μm]	σ_e [MPa]	t_m/t_c	σ_e / σ_c
A15-Al300	275	420	6	300	95	1.09	0.23
*A7-Al300	75	340	7.6	300	95	4.00	0.28
A5-Al300	175	350	8.7	300	95	1.71	0.27
*A9-Ni300	125	356	9	300	300	2.40	0.84
A15-Al150	275	420	6	150	95	0.55	0.23
A3-Al150	475	290	3	150	95	0.32	0.33
A3-Al100	500	290	3	100	95	0.29	0.33
A16-Al100	350	339	5.4	100	95	0.30	0.28
A4-Al100	225	380	3	100	95	0.44	0.25
A4-Al50	225	380	3	50	95	0.22	0.25
Z12-Al300	100	725	9.2	300	95	3.00	0.13
*Z12-Ni300	100	725	9.2	300	300	3.00	0.41
Z10-Ni150	300	750	8.6	150	300	0.50	0.40
Z10-Ni100	300	750	8.6	100	300	0.33	0.40
Z11-Al150	200	698	5.2	150	95	0.75	0.14
Z3-Al150	300	728	6.4	150	95	0.50	0.13
Z3-Al100	300	728	6.4	100	95	0.33	0.13
Z3-Al50	300	728	6.4	50	95	0.17	0.13
Z6-Al100	400	780	9.2	100	95	0.25	0.12
Z6-Al50	400	780	9.2	50	95	0.125	0.12

*Shaded areas indicate multiple cracking

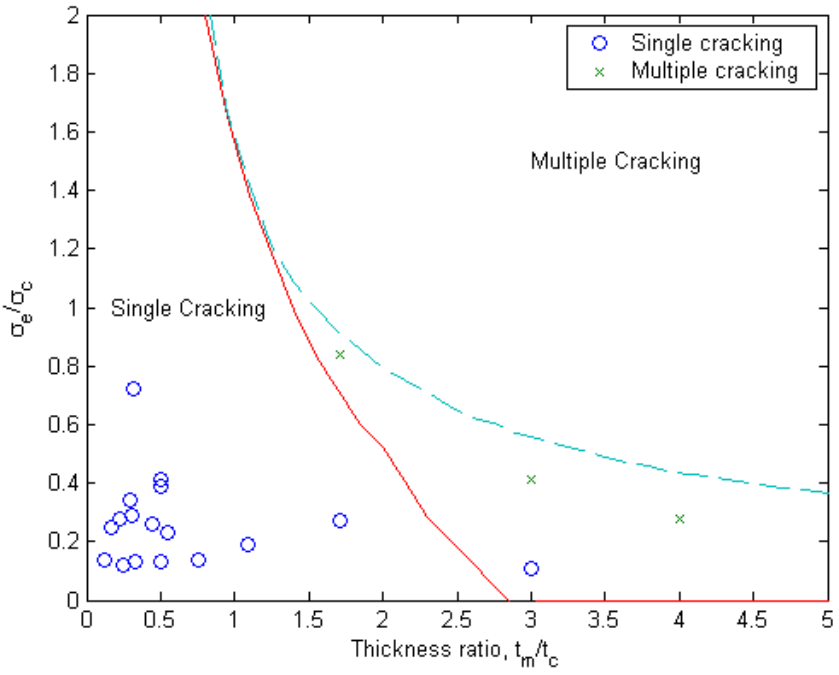

Fig. 13 Comparison between the composite fracture map and the experimental results.

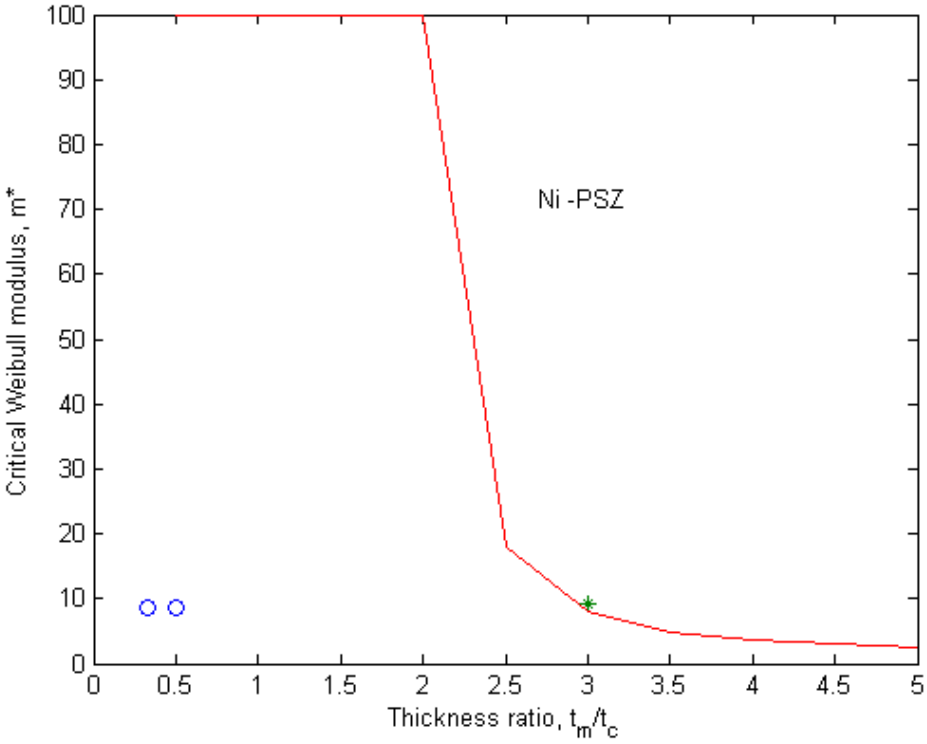

a)

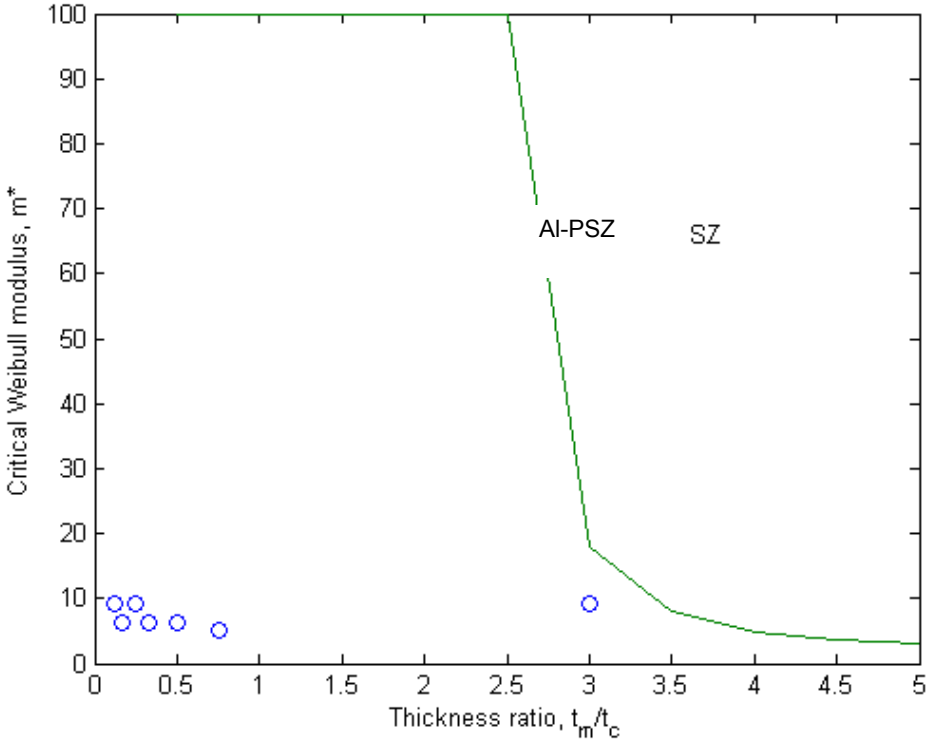

b)

Fig. 14 Comparison between the probability-based fracture map and the experimental results for PSZ bonded to: a) Nickel and, b) Aluminium

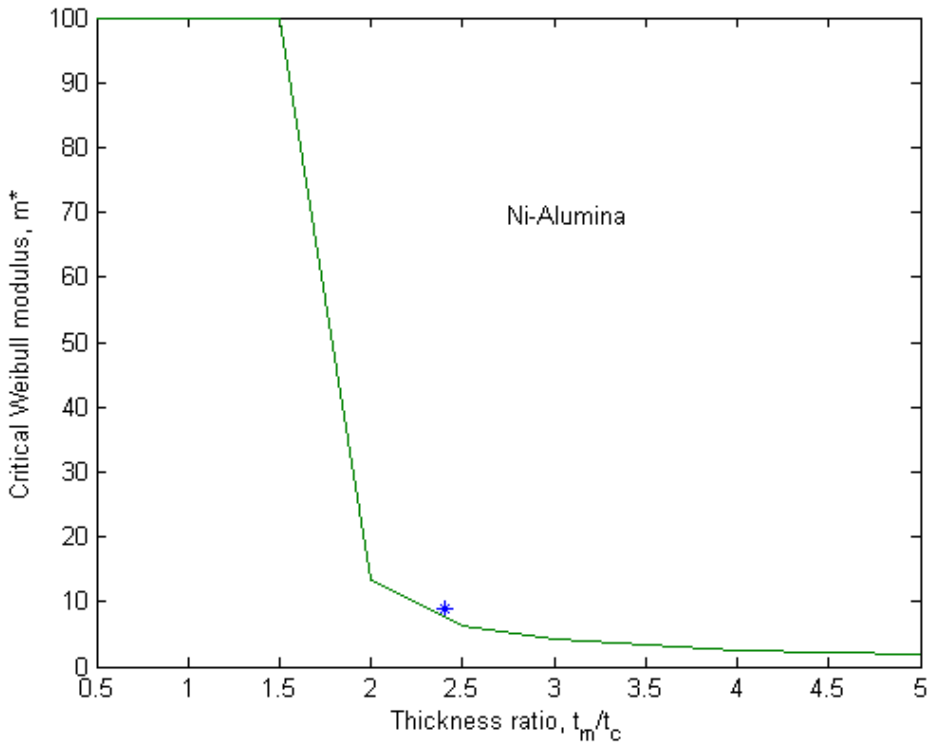

a)

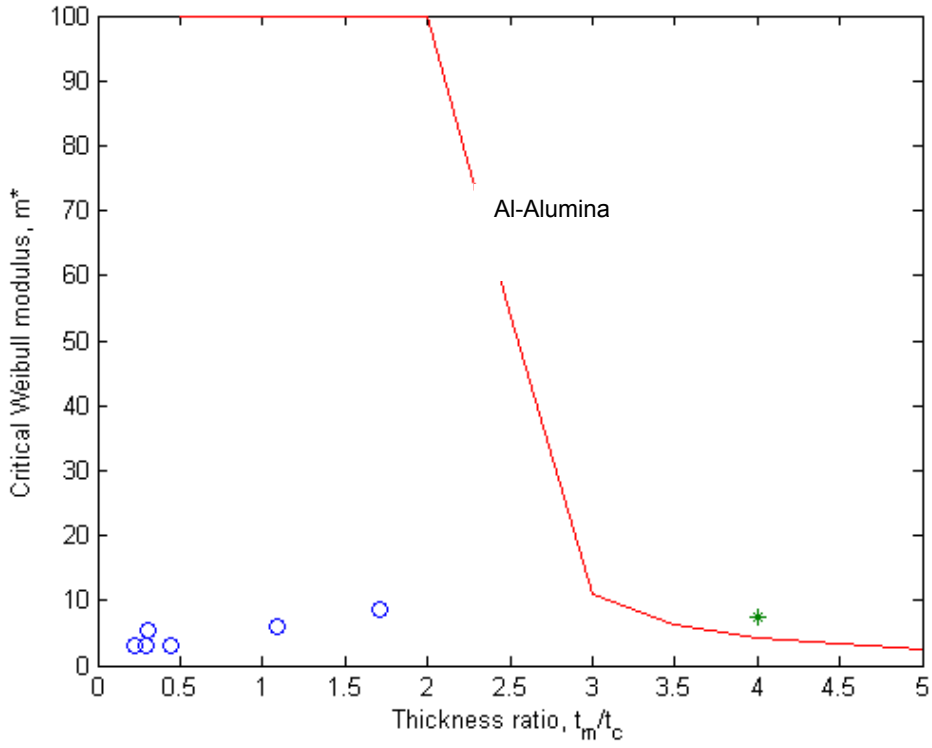

b)

Fig. 15 Comparison between the probability-based fracture map and the experimental results for Alumina bonded to : a) Nickel and, b) Aluminium